3d printing and testing of rose thorns or limpet teeth inspired anchor device for tendon tissue repair

Acta of Bioengineering and Biomechanics
Vol. 23, No. 4, 2021

Original paper
DOI: 10.37190/ABB-01899-2021-01

3D printing and testing of rose thorns or limpet teeth inspired anchor device for tendon tissue repair

MARIANA RODRIGUEZ REINOSO[1], MARCO CIVERA[1]*,
VITO BURGIO[1], FEDERICA BERGAMIN[2], OLIVER GRIMALDO RUIZ[1],
NICOLA MARIA PUGNO[3, 4]*, CECILIA SURACE[1]*

[1] Laboratory of Bio-Inspired Nanomechanics, Department of Structural,
Building and Geotechnical Engineering, Politecnico di Torino, Turin, Italy.
[2] Department of Hand, Plastic and Reconstructive Surgery, Ivrea Hospital, Ivrea, Italy.
[3] Laboratory of Bio-inspired, Bionic, Nano, Meta Materials and Mechanics,
Department of Civil, Environmental and Mechanical Engineering, University of Trento, Trento, Italy.
[4] School of Engineering and Materials Science, Queen Mary University of London, London, United Kingdom.

Purposes: Advancements in medical technology have enabled medical specialists to resolve significant problems concerning tendon injuries. However, despite the latest improvements, surgical tendon repair remains challenging. This study aimed to explore the capabilities of the current state-of-the-art technologies for implantable devices. *Methods*: After performing extensive patent landscaping and literature review, an anchored tissue fixation device was deemed the most suitable candidate. This design was firstly investigated numerically, realizing a Finite Element Model of the device anchored to two swine tendons stumps, to simulate its application on a severed tendon. Two different hook designs, both bio-inspired, were tested while retaining the same device geometry and anchoring strategy. Then, the applicability of a 3D-printed prototype was tested on swine tendons. Finally, the device-tendon stumps ensemble was subjected to uniaxial tensile tests. *Results*: The results show that the investigated device enables a better load distribution during the immobilized limb period in comparison to standard suture-based approaches, yet it still presents several design flaws. *Conclusions*: The current implantable solutions do not ensure an optimal result in terms of strength recovery. This and other weak points of the currently available proposals will serve as a starting point for future works on bio-inspired implantable devices for tendon repair.

Key words: *tendon and ligament injuries, tendon repair, sutureless, bio-inspired design, implantable medical device*

1. Introduction

Tendon and Ligament Injuries (TLIs) are, unfortunately, not an uncommon issue. On the other hand, surgical tendon repair remains challenging despite numerous advances in orthopaedic surgery. Current treatment strategies fail to restore the functional, structural and biochemical properties of repaired tendons. Although progress on this subject has been achieved, there is currently a high rate of occurrence for several complications during the recovery, mostly due to the limits of the current solutions.

Among all, suture threads (of various materials and realised with different passage and anchorage techniques) remain the vastly predominant approach. The major concerns about these conventional suture-based approaches are: (i) the formation of adhesions between healing tendon and surrounding tissues (with excessive formation of extrinsic scar tissue, predomi-

* Corresponding authors: Marco Civera, Department of Structural, Building and Geotechnical Engineering, Politecnico di Torino, Corso Duca degli Abruzzi 24, Turin, Italy. ORCID: 0000-0003-0414-7440. Phone: +39 011 090 4911, e-mail: marco.civera@polito.it; Nicola Maria Pugno, Department of Civil, Environmental and Mechanical Engineering, University of Trento, Via Calepina, 14, Trento, Italy. ORCID: 0000-0003-2136-2396. Phone: +39 0461 282525, e-mail: nicola.pugno@unitn.it; Cecilia Surace, Department of Structural, Building and Geotechnical Engineering, Politecnico di Torino, Corso Duca degli Abruzzi 24, Turin, Italy. ORCID: 0000-0003-2344-6948. Phone: +39 011 090 4904, e-mail: cecilia.surace@polito.it

Received: August 3rd, 2021
Accepted for publication: November 26th, 2021

nantly in small tendons, which limits the active range of motion), (ii) the inadequate grasping of the tendon by the suture causing slippage, (iii) knot failures, (iv) excessive gap formation (>3 mm), (v) insufficient tensile strength with potential rupture, and (vi) a high infection risk [15], [19], [29], [45]. Besides, medical conditions, including diabetes, circulation problems or obesity, may affect surgery outcomes [11]. Indeed, recent randomized controlled trials and observational studies on large tendons, such as the Achilles tendon, indicate that after surgical treatment, the complication rate is still high, regardless of the type of therapy, with a rupture rate ranging from 5% to 7% [6], [31]. Similar results were also reported for small tendons. In particular, after the flexor tendon repair (the second tendon injury with the highest incidence), the rate varies between 1% to 10% [8], [42]. In Italy, opinion experts have provided recommendations and guidelines about the treatments and rehabilitation of Achilles tendon injuries, based on scientific evidence and clinical experiences [32]. However, the same experts reported how the level of satisfaction achieved after Achilles tendon repair is generally unsatisfactory, concluding that there is not yet a clear solution to restore tendon strength and native function.

It is important to recall that different tendons possess unique anatomy, function, biomechanical properties, healing capacities, mechanisms of injury and approaches to rehabilitation. Furthermore, they may undergo degenerative and traumatic processes, with different outcomes. The most common injuries involve the rotator cuff, Achilles, and hand flexor tendons. However, despite anatomical and size differences among tendons, according to their locations, any solution considered for surgical treatment (sutures, barbed sutures, implantable devices) must follow some common considerations. The ideal solution should have suitable tensile strength and Young's modulus of elasticity to mimic the pristine tendon mechanical behaviour. It should respect the tendon biological and biomechanical functions and enable early postoperative rehabilitation; indeed, early motion is crucial after tendon repair surgery to promote intrinsic tendon healing while reducing extrinsic adhesion formation and preventing joint stiffness [44]. Specifically for implantable devices, all these aspects require a proper definition of their optimal geometry and anchoring strategy.

This study aimed to demonstrate the functioning of an implantable anchor device for tendon tissue repair. Rose thorns and limpet teeth inspired barbs were considered.

2. Materials and methods

2.1. Tendon mechanical properties

The mechanical behaviour of a tendon repair solution should match as closely as possible the one of the pristine tissue, without being too flexible nor too stiff. An excessively flexible device undergoes an uncontrolled elongation, whereas a constant diastasis <2 mm between the tendon's stumps is needed to ensure tissue healing [35]. On the other hand, a rigid device causes a disproportionate accumulation of mechanical stress in the anchoring areas, causing local tissue damage and potentially its mechanical failure.

In this sense, the tendons are composed of a hierarchical structure based on collagen fibrils subunits arranged in aligned fibres that are organized longitudinally into fascicles [41]. The main role of the fibres is to resist stress, allowing a certain degree of compliance (i.e., reversible longitudinal deformation). Due to the distribution of those aligned fibres through a matrix, the tendon mechanical behaviour may be realistically considered as an orthotropic material, whose elastic modulus is from 350 to 850 MPa (longitudinal direction) and from 1 to 40 MPa (transverse direction), where the variation in values is related to anatomical locations [37]. In general, the ultimate tensile strength (UTS) of tendons varies in the range of 30–45 MPa with an elongation percentage of 14–18% for children and young people; for adult tendons, UTS is between 43 and 115 MPa with an elongation percentage of 10–12.5% [17]. For the numerical and experimental analyses reported in this study, the mechanical properties of the flexor digitorum profundus (FDP) tendon were considered. Specifically, it was assumed that the device must be able to sustain at least the physiological values of the uniaxial tensile load expected during the active rehabilitation process (19 N, according to [38]).

2.2. Selection of the device geometry and anchoring strategy

An extensive search was performed on EspaceNet and Google Patent, focusing on patents for implantable devices for tendon repair. This first, broader research returned a total of 699 patents, involving several technology domains and considering any geographical region, CPC class, publication date, and assignee(s). This group was narrowed to 29 by considering only

Table 1. Shortlist of candidate patents

Patent number	Name	Assignee	Classification
US9,149,354B2	Flexor tendon repair device	Anthony E. Sudekum	A6F 2/00, A6B 7/06, A6IB 7/II, A6IF2/08
US20050119694A1	Remotely anchored tissue fixation device and method	Coapt Systems Inc.	A61B17/11
US20090228022A1	Device and method for tendon, ligament or soft tissue repair	Mcclellan William Thomas	A61B17/1146
US5916224A	Tendon repair clip implant	US Secretary of Army	A61B17/1146
US5723008A	Splint for the repair of tendons or ligaments and method	Gordon Leonard	A61B17/1146
US20130013065A1	Tendon repair device and method	INNOSPAN	A61B17/1146
US5800544A	Tendon and ligament repair system	Omeros Medical Systems Inc.	A61F 2/08
US3842441A	A temporary implant and method for tendon surgery	A. Kaiser	A61F 2/08
US20050197699A	Tissue repair apparatus and method	Coapt Systems Inc.	A61F 2/08

patents that specifically included the rems "tendons" and "ligaments" in their claims (21 out of 29) or other sections of their text (8 out of 29). Indeed, this study focused on implantable devices since they are supposed to overcome the well-known limitations of both classic and knotless approaches, such as (1) being applicable with non- or minimally invasive procedures, (2) being sutureless – thus less prone to mechanical failure thanks to the larger cross-sectional area, (3) being bioabsorbable, (4) ensuring a more uniform distribution of loads, and (5) being overall easier to apply.

After a critical review of the remaining candidates, the final shortlist reported in Table 1 was defined. A comparison among these potential solutions is graphically displayed in Fig. 1, considering the five beneficial characteristics enlisted before and a scale from 1 to 4, where 1 means it lacks that property and 4 means it completely fulfils it.

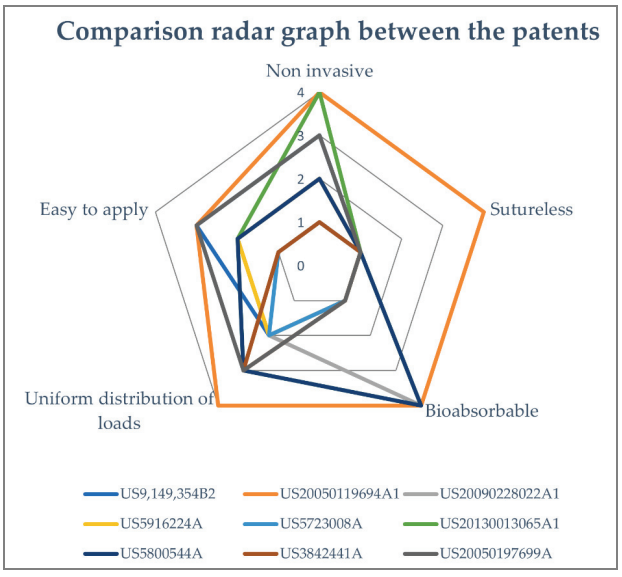

Fig. 1. Patent comparison graph

In conclusion, the US20050119694A1 patent was deemed as the most suitable option. According to the Authors' considerations, its principal advantages are: (i) its innovative micro-structured geometry that enables natural tissue imbibition; (ii) the anchorage system that ensures a uniform stress distribution during its application; finally; (iii) its biodegradability strongly reduces inflammatory response issues, as a result of being bioresorbable during the healing process. Besides, the US20050119694A1 patent was considered for its similarity with barbed sutures. Several studies have shown that barbed sutures have optimal mechanical behaviour in comparison with classic threads [7]. The device (Fig. 2) is made up of two thin patches or membranes, with a plurality of barbs disposed on the interior side. These latter ones constitute the micro-structured anchorage system surface that holds the device to the target tissue. The distance between the two opposite sets of rows is intended to avoid anchoring on the damaged portion of the tendon. Indeed, differently from the straight cut introduced here for these experiments, generally large tendons (e.g., Achille's tendon) reach collapse due to mechanical fatigue. This means that the severed cross-section is actually surrounded by a portion of tendon tissue that may be partially damaged; thus, anchoring in these nearby areas may (1) provide non-optimal anchoring and (2) potentially cause further damage.

This patent was considered a viable option for several reasons. The main aspects were that: (1) its two thin membranes can be anchored to the upper and lower tendon surfaces, leaving uncovered the lateral parts of the tendon, enabling the natural imbibition of the tendinous tissue (differently for other solutions which are completely wrapped around the tendon); (2) the orientation of the two sets of barbs allowed for optimal tensile resistance coming from the two tendon stumps;

(3) the gap left between the two series of anchorage barbs ensured that the tendon stumps near the injury area are not stressed to avoid the problem of scar tissue formation. However, further improvement of the design retrieved from the existing literature was considered, including some modifications to the barbs arrangement and shape. Regarding the barb shapes, two variants were considered, following a biomimetic approach inspired by a rose thorn (0.45 × 0.45 × 0.7 mm) and a limpet tooth-like [2] (0.55 × 0.4 × 0.94 mm) shapes (Fig. 3), owing to their natural grasping function.

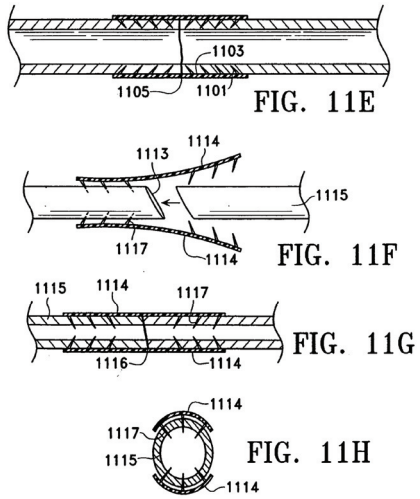

Fig. 2. Patent US20050119694A1 (retrieved from [43])

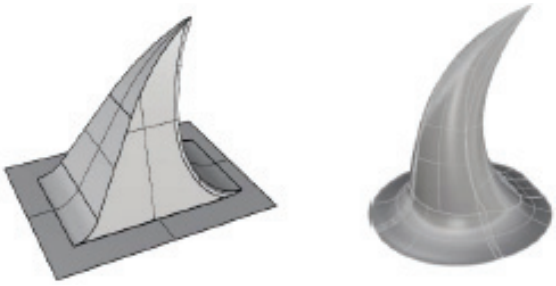

Fig. 3. Detail of a single barb. Rose torn- (left) and limpet tooth-inspired (right) shapes

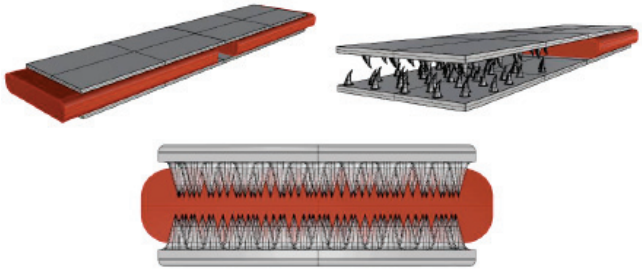

Fig. 4. CAD model of the implantable device, with two membranes (Patches) with barbs arranged in a checkerboard pattern on their interior side. The red solids indicate the two (distal and proximal) tendon stumps

As can be seen in Fig. 4, the barbs were arranged in a checkerboard pattern. This was done considering the tendons' hierarchical fibre structure along its longitudinal direction. The rationale was that by inserting all barbs aligned in the same rows, they should have been all anchored on the same fibres, overloading them.

For the same reason, the barb distribution is inverted onto the two membranes. This way, they do not anchor on different fibres. Moreover, the barb tips of both sides of the device do not come into contact during insertion.

2.3. Candidate biomaterials

As mentioned in Section 2.2, the implantable device is supposed to be biocompatible and biodegradable. Exhaustive research was conducted to find the right polymeric material.

Several biopolymers can be found in the scientific literature, but not all of them are biodegradable. Another important parameter is the degradation time because it must match with the healing time of tendon tissue. Thus, the degradation process of the polymeric material must start around the sixth month to guarantee a complete formation of new tissue [36]. Biomaterials that did not satisfy this requirement were discarded. In Table 2, the polymeric materials suitable

Table 2. Mechanical properties for different polymers

Material	PGA	PLA	PCL
Density [g/cm^3]	1.5–1.7 [10], [26]	1.21–1.3 [10]	1.11–1.146 [10]
Young's Modulus [GPa]	6–8.4 [10], [26]	0.35–13.8 [10], [24], [27]	0.21–0.44 [10]
Poisson's coefficient	0.3 [10]	0.36 [10]	0.3 [33]
Yield strength [MPa]	–	16–103 [27]	8.2–10.1 [9]
Elongation at break	1.5–30% [3], [10], [18], [26]	6–7% [1]	300–1000% [10]
Tensile strength [MPa]	60–99.7 [10]	50–70 [1]	4.0–42 [10], [18]
Compression strength [MPa]	–	17.9–93.8 [5]	–
Flexural strength [MPa]	–	61.8–94.7 [27]	–
Tensile breaking load [MPa]	55–890 [18], [23], [26]	16–114 [27]	10.5–16.1 [9]
Degradation times [Months]	6–12 [3], [22], [47]	6–18 [12]	>24 [3], [47]

for the goal of this study (medical-grade polylactic acid (PLA), polyglycolic acid (PGA), and polycaprolactone (PCL) are illustrated. Their respective ultimate stress and Young's modulus were reported for comparison. These three alternatives were then tested numerically to find the best candidate (Section 3.1).

Among these options, the PLA was presumptively considered the most probable choice, due to its Young's modulus. In fact, an elastic modulus in the range of 1–2 GPa is optimal. This consideration was made to avoid excessive stress concentration or elongation during loading. If the polymeric material had too high stiffness, a high rate of stress was situated in the tendon tissue near the contact zone; otherwise, a material with low Young's modulus broke or underwent too large deformations.

2.4. Numerical investigation: the finite element analysis (FEA)

The aims of both the numerical and the experimental tests were to verify (1) the bio-inspired, microstructured anchorage system and (2) the tendon stumps-implantable devices ensemble. Specifically, the whole device at its global scale and the single barb must be able to resist the physiological loads expected during the post-operative rehabilitation process (active and passive motion). The finite element analysis (FEA) was performed using the ANSYS® Mechanical Workbench™ software, importing CAD models developed using the Rhinoceros® software. A free mesh of TED10 10-node tetrahedral elements [20] was applied for all the structures with 414 243 elements in the upper membrane, 413 934 in the lower membrane, 234 155 in the proximal tendon stump and 234 996 in the distal tendon stump. This enabled reproducing the curved surfaces and edges properly. A non-separation nonlinear contact was imposed between the tendon and device surfaces. In Table 3, the mechanical parameters considered for the FE tendon model are reported. For the reasons explained in section 2.1, a linear elastic orthotropic behaviour was assumed. To model the size and geometry of the two tendon stumps, it was considered that the adult FDP tendon has a cross-section area of 19 ± 6 mm^2 in correspondence with the metacarpophalangeal annular pulley A1 [46]. For the design of its geometry, a ratio of 1:5 was maintained between thickness and width.

Table 3. Mechanical parameters for the elastic orthotropic tendon model [37]

Poisson's ratio [–]	0.350
Fibril modulus [MPa]	1.70
Matrix modulus [MPa]	1.00
E_1 [MPa]	4.75
E_2 [MPa]	4.75
E_a [MPa]	962.99
V_{12} [–]	0.253
V_{13} [–]	0.023
V_{23} [–]	0.023
G_{12} [MPa]	1.18
G_{13} [MPa]	45.64
G_{23} [MPa]	45.64

This static analysis (Fig. 5) assumed one of the tendon stumps proximal to the tendon-bone junction and considered it acting as a fixed support. The other

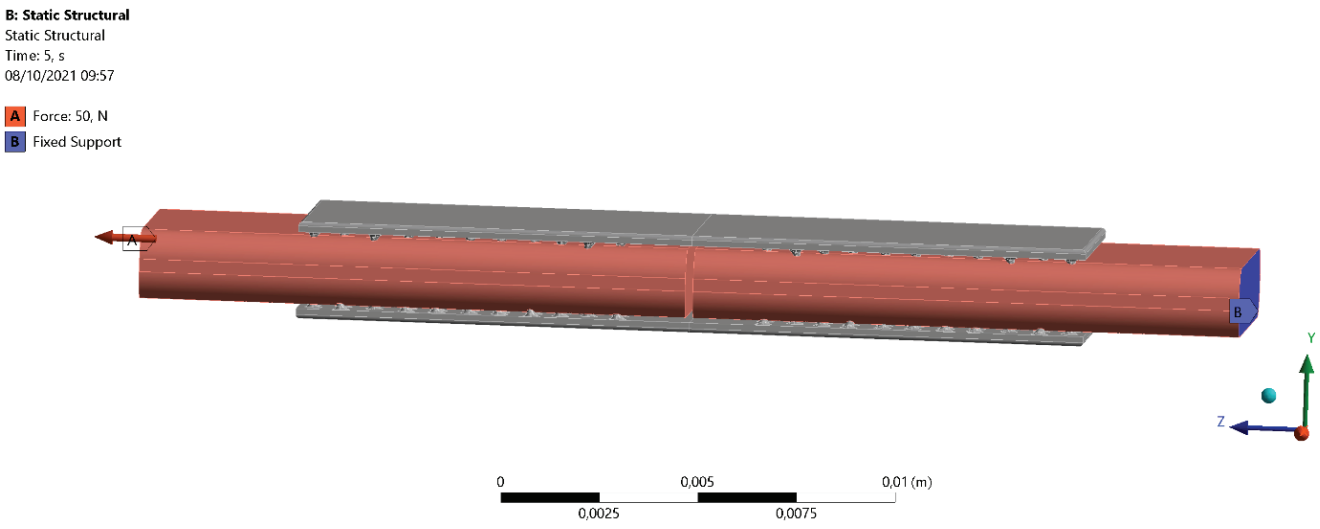

Fig. 5. Boundary conditions: a fixed support was applied on the distal surface of the first tendon stump that mimics the tendon-bone junction, with the axial force applied to the other tendon stump

stump, consequently assumed to be proximal to the myotendinous junction, was subjected to an axial load of 50 N, representing the muscular force transmitted during finger flection. This is known to exert a force in the range of 40–50 N during active movement [7].

The mechanical properties of the device depended on the selected biopolymer. According to the range of values reported in [10] and in Table 2, a density ρ of 1.25 g/cm^3, Young's modulus E of 2.00 GPa, and a Poisson's ratio v of 0.360 were considered for PLA. For PGA, ρ = 1.60 g/cm^3, E = 8.40 GPa, and v = 0.300 were set. For PCL, ρ = 1.13 g/cm^3, E = 0.44 GPa, and v = 0.300 were utilised.

2.5. Experimental investigation

2.5.1. Device manufacturing

Several manufacturing technologies were considered to find the production techniques that make it possible to accurately model the geometry of the device. Additive manufacturing in general, FDM and the Photopolymer Jetting 3D-printing technology in particular were deemed as the most suitable options considering the selected material and the geometric accuracy required. However, the commercially available FDM 3D printers use non-medical-grade biopolymers that have different mechanical properties than their counterparts of interest here. Moreover, even if the accuracy of this technology reaches a layer height of 100 µm, it is still not satisfactory, as the smallest details of the geometry designed in the CAD software cannot be well replicated. Thus, an Objet30 3D-printer, with Polyjet® technology, was used. This allowed for high manufacturing accuracy (almost 15 micrometres). Among the resins available for this printer, the VeroWhite Plus RGD835 was considered as the most appropriate owing to its PLA-like mechanical properties: elastic modulus E = 2.00 GPa and ultimate tensile strength equal to 65 MPa [40], very close to the values generally considered for PLA (50–70 MPa [1]). In Figure 6, an example of the printed device is shown.

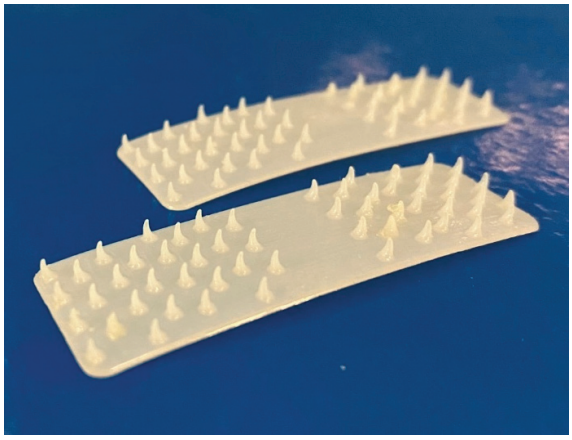

Fig. 6. 3D-printed devices (limpet tooth-inspired shape, VeroWhite Plus RGD835 resin)

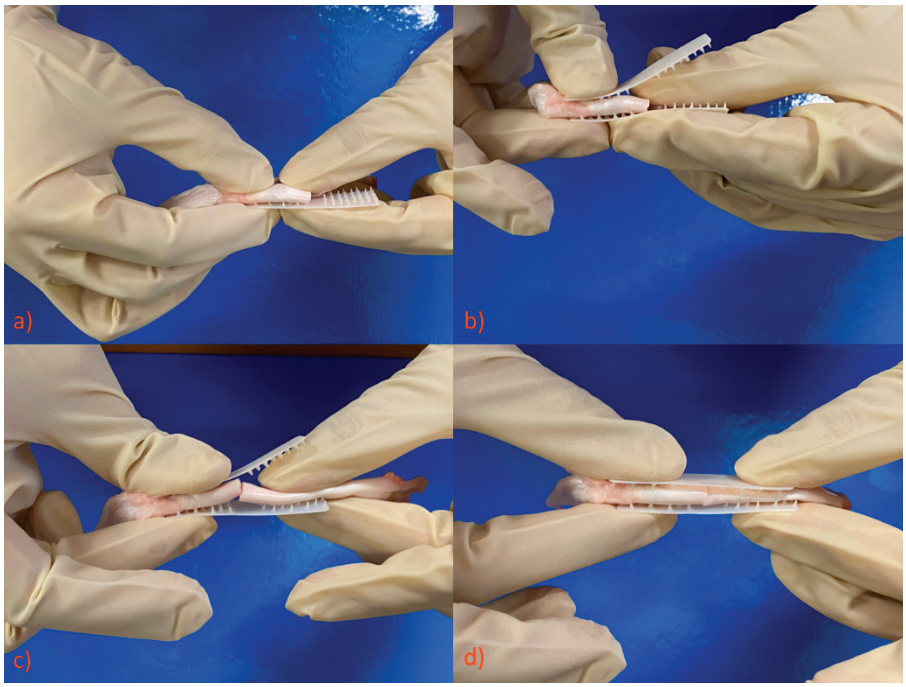

Fig. 7. The four-steeped application process: a) first tendon stump grasping, b) first tendon stump upper surface grasping, c) second tendon stump grasping, d) second tendon stump upper surface grasping

The selected resin was intended for laboratory tests only. This material, while biocompatible, is not intended for the manufacturing of implantable devices, also due to its high moisture absorption (over 1%) [30].

2.6. Swine tendon samples

The porcine deep flexor tendons have been used as a model for the human tendon, as suggested by the scientific literature ([4], [14], [21], [28], [39]). The similarities in strength and size between swine FDP and human hand flexor tendons have been deeply utilised for tendon repair studies [25]. The FDP tendons were extracted from six disarticulated anterior swine trotters. Importantly, only recently slaughtered pigs were employed. Fresh (not frozen) FDPs extracted from recently slaughtered swine specimens were used to ensure unaltered biological conditions. The technique described in [17] for FDP harvesting was followed. The skin, subcutaneous tissues, and FDS were excised. Finally, the FDP tendons were isolated and extracted. Subsequently, a tendon injury was simulated by making a transverse cut, dividing each tendon into two separate stumps.

2.7. Tendon stumps-device ensemble

The application process presented in Fig. 7 consists of the following steps. First, one tendon stump was snagged on the multiple sites for grasping on the lower supportive backing component; subsequently, the upper component was applied on the upper surface. The application process was repeated for the second tendon stump, considering having the minimum gap between them.

3. Results

3.1. Numerical analysis

Two parameters were deemed as the most relevant in this study: the equivalent (von Mises) stress, to verify that the maximum mechanical stress was below the ultimate resistances of the tendon stump tissue and the device, and the u_z axial displacement, essential to verify whether the diastasis between tendon stumps increase during the load since, as mentioned before, optimal healing of the tissue occurs if diastasis remains constantly smaller than 2 mm. The results shown in Table 4 were obtained for the two bioinspired barb designs.

Table 4. Maximum von Mises stress and u_z displacements for the two barb geometries

Von Mises Stress [MPa]			Displacement u_z [mm]		
Model	Patch max.	Tendon max.	Model	Patch max.	Tendon max.
Rose thorn	70	80	Rose thorn	0.11	0.10
Limpet teeth	38	91	Limpet teeth	0.12	0.13

By comparing the two designs, it is evident that the limpet teeth shape returns the best mechanical response

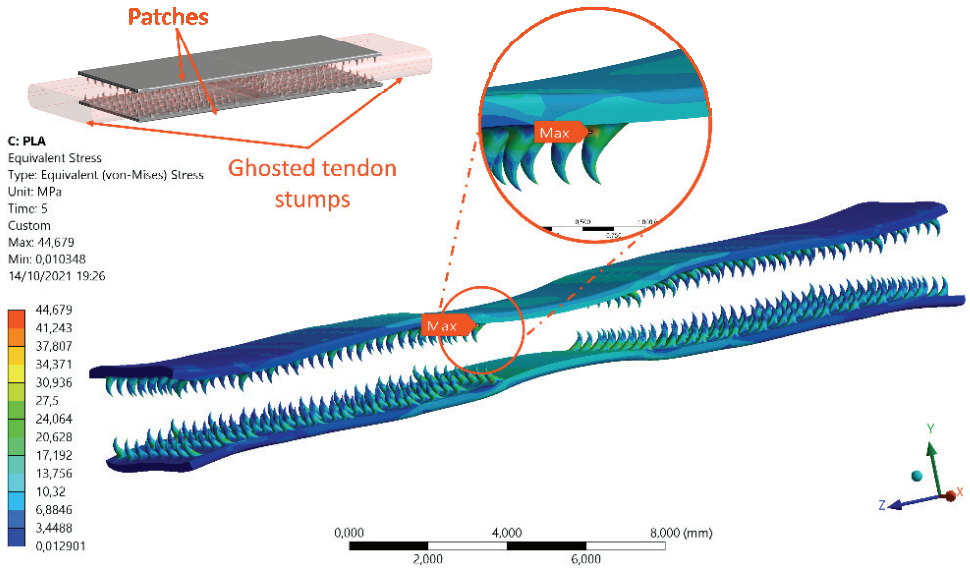

Fig. 8. Von Mises stress distribution throughout the patch (limpet teeth-like shape).
The tendon stumps are ghosted for better visibility; the shape of the membranes is shown as deformed under the applied load

in terms of lower maximum stress in both the two patches and the tendon stumps, even if at the cost of a slightly larger axial displacement (which is still well under the threshold considered here). Therefore, only this second design was considered for the second phase (i.e., the experimental tests). In Figure 8, the simulation results for this design is shown. As expected, the maximum tensile stress was found at the base of the barbs in the row closest to the severed tendon cross–section.

At the same time, the equivalent stress is almost uniformly distributed throughout the device. This highlights the capabilities of the microstructured anchoring system to reduce the stress accumulation at one or a few points, differently from the (barbed or classic) suture threads, thus avoiding local damage and/or failure to the tendon fibrillar structure.

These preliminary numerical analyses brought satisfactory results; however, by looking at the distal part of the device, it can be observed how the last few barb rows do not grip the tendon stumps. This is due to the deflection of the device during loading. Experimental validation was deemed necessary to address this specific issue.

In addition, two other numerical simulations have been made using the other candidate biomaterials reported in Table 2 (PGA and PCL).

Finally, PLA was identified as the most suitable option, due to its mechanical properties (see its lower maximum von Mises equivalent stress in Table 5), its degradation time, and also considering its well-known extensive use for the manufacturing of medical implants.

Table 5. Maximum von Mises stress for different biomaterials

Maximum von Mises stress [MPa]		
	Patch	Tendon
PLA	44.68	34.15
PGA	62.69	33.66
PCL	47.40	65.21

3.2. Experimental tests

3.2.1. Insertion test

The first test aimed at establishing the feasibility of the application procedure, as shown in Fig. 7. The aspects considered were: (1) the easiness of penetration through the tendon tissue; (2) a visual inspection of the structural integrity of the device after compression; (3) a visual inspection of the structural integrity of the surrounding biological tissues after insertion. The device with limpet teeth-like barbs successfully passed this phase. These were only preliminary tests. For more reliable results, cadaver tests are needed, with the device implanted under the skin while performing passive mobilization of the limb.

3.2.2. Tensile test of the device-tendon ensemble

Uniaxial tensile tests were carried out according to the UNI EN ISO 527 standard, with an MTS INSIGHT® machine set as follows: 1000 N load cell, speed of 0.3 mm/s, and a sampling frequency of 20 Hz.

Since the experimental validation was performed on swine tendon specimens (to avoid using human tissues), it was considered that the ultimate stress for the FDP tendon is 55 ± 19 MPa [34]. This was set as the holding power that the tendon stumps-device ensemble should ideally provide.

During traction of the tendon-device ensemble, the distal barbs of the device started decoupling from the tendon stumps due to deflection because of load application. This confirmed the risk of unhooking suggested by the numerical analysis reported in Fig. 8. This phenomenon was observed after the application of relatively small loads, which can naturally occur during the active rehabilitation process, thus, invalidating all the operating principles of the anchorage system. Importantly, the peak uniaxial tensile load value (6.44 N) was lower than the threshold defined according to these expected physiological values (19 N as explained previously in Section 2.1). This issue can be even worsened in real-life scenarios, where more complex movements could also involve shear forces acting on the device.

The maximum load attained with the original design was limited because of the unlocking of the teeth at the distal ends. To increase the holding power, the ends of the device were tethered. By fixating the ends, the maximum load was increased but at the cost of modifying (complicating) the design. Two bands were positioned in the distal and proximal portions of the device. This avoided completely the unhooking problem; it might be also considered feasible in a surgical procedure, even if not ideal due to the need for a further step when operating in a small, sensitive environment. However, even in this case, the peak load value (18.49 N) was still lower than the considered threshold (even if only by a small margin). In Figure 9a, the initial positioning of the tendon-device ensemble during the tensile tests is shown. The device deflection and consequential unhooking are clearly visible

in the box in the bottom right corner. In Figure 9b, the same tests when performed on the device with the two bands are shown.

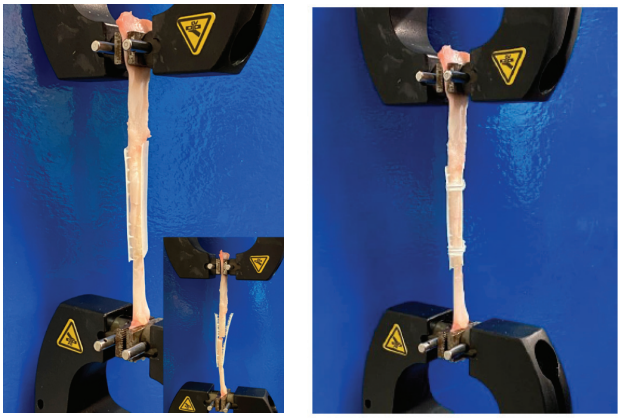

(a) (b)

Fig. 9. (a) Tensile test of the device inserted on swine tendons stumps and the deflection of the device by applying small loads; (b) Tensile test of the device with two bands

In Figure 10, an example of a load [N] – extension [mm] curve as obtained from the uniaxial tensile tests is shown (both configurations, with and without bands, are reported). These experimental results highlight how the device cannot stand the physiological load presented during passive rehabilitation, thus losing its final purpose.

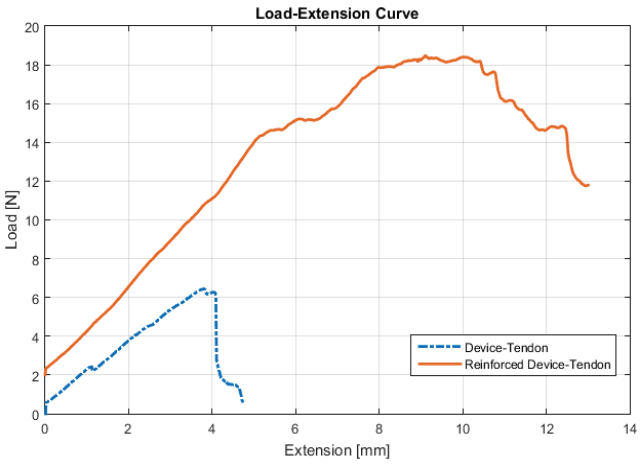

Fig. 10. Load – extension curve for the device-tendon stumps ensemble with (solid red line) and without (dot-dashed blue line) the constraining bands

4. Discussion

The finite element analysis highlighted how the use of a plurality of hooking microstructures makes the stress distribution more uniform. Therefore, it successfully eliminates the concentration of stresses which characterizes suture threads.

During the insertion test, it was observed that the system has good penetration capacities, piercing the tendon tissue without encountering much resistance. The manageability during the application of the device is optimal; its application is not very complicated even for an inexperienced user.

However, both numerical simulations and experimental tests evidenced the bowing of the two patches when the tendon is subjected even to small uniaxial tensile loads.

This bowing behaviour tends to unhook the distal parts of the device, thus invalidating the principle of operation of the device. The insertion of two bands as an additional constraining element in the distal portions of the device increases the holding power of the device-tendon ensemble by three times. However, even in this latter case, the failure mechanism was the results of unhooking of the two patches from the tendon stumps. The holding power was found to be lower than both the ideal target values (~55 MPa) and the performance of non-implantable direct competitors.

As discussed in Section 2.2, the tested patent was chosen because of the similarity of its anchoring strategy with barbed suture threats. However, by making a comparison between the holding power of both technologies, it stands out that barbed suture threats reach a holding power of 50.3 ± 9.9 N for 2/0 polypropylene QuillTM SRS 4-strand technique and 61.5 ± 11.0 N with a 2/0 polydioxanone (PDO) QuillTM SRS with the same 4-strand technique [7], while the tested device reaches only 5 N.

This result is also overperformed by other more classic suture-based solutions. Several comparative studies of traditional suturing techniques have shown that the maximum tensile load for those techniques are: Kessler 20 N; Becker 20.7 N; Savage 37.1 N; Modified Kessler + epitendinous running suture 33.6 N; Modified Kessler + Halsted's epitendinous suture 48.04 N; "Six strands" of Savage 67.17 N; "Interlocking" (as proposed by Robertson & Al-Qattan) 36.17 N; "Cross-stitch" (as proposed by Silfverskiöld and Andersson) 34.9 8 N, and the epitendinous simple running suture 19.6 N [13], [48]. These all exceed the maximum resistance obtained with the tested device, both with and without the additional bands.

These findings point out that the functional principle of the hooks is theoretically valid, yet several aspects, such as the barb distribution, should be further improved to increase the anchoring power.

5. Conclusions

This study aimed at evaluating the feasibility of the current proposals for implantable medical devices for tendon repair. Specifically, based on a preliminary, extensive patent landscape, the best candidate concept was selected. This was made up of two superposed thin patches, with a plurality of barbs arranged in the inside of the upper and lower patches. This was deemed as a valid concept since it ensures the natural imbibition of the tendon tissue while anchoring two regions of tissue together, with a more uniform distribution of the tensile stress over a large surface.

The original concept was then improved considering a different arrangement of the barbs and two candidate barb designs (inspired by rose thorns and limpet teeth specifically). These modified versions were both evaluated numerically.

The evaluation was performed with three types of analyses: (1) numerical simulations on a Finite Element Model, (2) an experimental device application test, and (3) ultimate tensile strength tests.

The Finite Element Analysis showed better results for the limpet teeth-like option, so only this design was tested experimentally as well. To accurately reproduce the geometry in the smallest details, Polyjet 3D printing was employed. The commercial resin VeroWhite Plus RGD835 was used since its mechanical properties PLA-like well match the ones from medical grade PLA. To produce a realistic model of the elastic behaviour of the FDP tendon, swine FDPs were considered, as usually done to study traditional techniques for hand tendon repair thanks to their well-known similarities to their human counterparts. In particular, fresh (not frozen) swine FDPs were used.

The insertion test verified the feasibility of using limpet teeth shape to penetrate the tendon tissue without excessive damage to the surrounding tissue. However, it did not return satisfactory results in the Uniaxial tensile tests, reaching only 6 N before failure. Even when supported by adding two external bands, the holding power tripled to 18 N but still remained below expectations.

Therefore, this study suggests how a barbed patches system is overall interesting and feasible from a manufacturing and insertion point of view, however, if manufactured with current medical grade materials, its performances are not competitive with already existing options. Even worse, it is not a functional solution for anchoring two tendon stumps during an active rehabilitation process. Its design flaws hamper its application for tendon reconstruction surgery if not coupled with suture threads.

These findings provide a useful starting point for research on new concepts for implantable devices for tendon and ligament repair. The stand-alone use of the barbed device is not valid since the barbs are unable to retain a stable anchoring between the tendon stumps during the active rehabilitation process. Nevertheless, this study also shows how a similar concept may be used to completely replace the suture thread if the unhooking issue encountered can be bypassed. Thus, it sets the conditions and the direction for designing new tendon repair devices, which is to be reported in future studies. Finally, the research reported here focused on the (1) geometry and (2) anchoring system of the implantable device. Future works need to focus on the material for the same application. Indeed, an implantable solution should be not only biologically inert, to avoid interference with the tendon healing process, but preferably bioabsorbable, to avoid the need for surgical removal after complete healing.

Conflict of interest statement

The Authors declare no conflict of interest.

Ethical approval

This study does not contain any studies with human or animal subjects performed by any of the authors.

Acknowledgements

The authors acknowledge Politecnico di Torino's Proof of Concept grant DR #402, 24th April 2018. The support received from our master's degree students in the collection, analysis, and interpretation of data is greatly appreciated.

References

[1] AURAS R., LIM L.-T., SELKE S.E.M., HIDETO T., *Poly(Lactic Acid) (Synthesis, Structures, Properties, Processing, and Applications)*, Mechanical Properties, 141–153, DOI: 10.1002/9780470649848.ch11.

[2] BARBER A.H., LU D., PUGNO N.M., *Extreme strength observed in limpet teeth*, J. R. Soc. Interface, 2015, 12 (105), 0–5, DOI: 10.1098/rsif.2014.1326.

[3] BUREAU I., *WO 2007/066339 Al Drug-delivering composite structures*, 2007.

[4] CAO Y., XIE R.G., TANG J.B., *Dorsal-enhanced sutures improve tension resistance of tendon repair*, J. Hand Surg Br., 2002, 27 (2), 161–164, DOI: 10.1054/jhsb.2001.0687.

[5] CHILSON L. (2013), *The Difference Between ABS and PLA for 3D Printing*, Available at: http://www.protoparadigm.com/newsupdates/thedifferencebetweenabsandplafor3dprinting/ (Accessed: July 2019).

[6] CLAYTON R.A., COURT-BROWN C.M., *The epidemiology of musculoskeletal tendinous and ligamentous injuries*, Injury, 2008, 39 (12), 1338–1344, DOI: 10.1016/j.injury.2008.06.021.

[7] CLEMENTE A., BERGAMIN F., SURACE C., LEPORE E., PUGNO N., *Barbed suture vs conventional tenorrhaphy: biomechanical analysis in an animal model*, J. Orthop. Traumatol., 2015, 16 (3), 251–257, DOI: 10.1007/s10195-014-0333-8.

[8] DY C.J., HERNANDEZ-SORIA A., MA Y., ROBERTS T.R., DALUISKI A., *Complications after flexor tendon repair: a systematic review and meta-analysis*, J. Hand Surg. Am., 2012, 37 (3), 543–551, DOI: 10.1016/j.jhsa.2011.11.006.

[9] ESHRAGHI S., SUMAN DAS, *Mechanical and microstructural properties of polycaprolactone scaffolds with one-dimensional, two-dimensional, and three-dimensional orthogonally oriented porous architectures produced by selective laser sintering*, Acta Biomaterialia, 2010, 6 (7), 2467–2476, DOI: 10.1016/j.actbio.2010.02.002.

[10] FARAH S., ANDERSON D.G., LANGER R., *Physical and mechanical properties of PLA, and their functions in widespread applications – A comprehensive review*, Adv. Drug Deliv. Rev., 2016, 107, 367–392, DOI: 10.1016/j.addr.2016.06.012.

[11] FRANCESCHI F., PAPALIA R., PACIOTTI M., FRANCESCHETTI E., DI MARTINO A., MAFFULLI N., DENARO V., *Obesity as a risk factor for tendinopathy: a systematic review*, Int. J. Endocrinol., 2014, DOI: 10.1155/2014/670262.

[12] GENTILE P., CHIONO V., CARMAGNOLA I., HATTON P.V., *An overview of poly(lactic-co-glycolic) acid (PLGA)-based biomaterials for bone tissue engineering*, J. Mol. Sci., 2011, 15 (3), 3640–3659, DOI: 10.3390/ijms15033640.

[13] GORDON R.P.L.L., TOLAR M., VENKATESWARA RAO K.T., RITCHIE R.O., RABINOWITS S., *Flexor tendon repair using a stainless steel internal anchor*, J. Hand Surg. Am., 1998, 23B (1), 37–40, DOI: 10.1016/s0266-7681(98)80215-5.

[14] HADDAD R.J., KESTER M.A., MCCLUSKEY G.M., BRUNET M.E., COOK S.D., *Comparative mechanical analysis of a looped-suture tendon repair*, J. Hand Surg. Am., 1988, 13 (5), 709–713, DOI: 10.1016/s0363-5023(88)80130-8.

[15] HANADA M., TAKAHASHI M., MATSUYAMA Y., *Open re-rupture of the Achilles tendon after surgical treatment*, Clin. Pract., 2011, 1 (4), 299–301, DOI: 10.4081/cp.2011.e134.

[16] HIRPARA K.M., ABOUAZZA O., O'NEILL B., O'SULLIVAN M., *A technique for porcine flexor tendon harvest*, J. Musculoskelet. Res., 2006, 10 (4), 181–186, DOI: 10.1142/S0218957706001856.

[17] IPPOLITO E., NATALI P., POSTACCHINI F., ACCINNI L., DE C.M., *Morphological, immunochemical, and biochemical study of rabbit achilles tendon at various ages*, J. Bone Joint Surg. Am., 1980, 62 (4), 583–598.

[18] JAMSHIDIAN M., TEHRANY E.A., IMRAN M., JACQUOT M., DESOBRY S., *Poly-Lactic Acid: Production, Applications, Nanocomposites, and Release Studies*, Compr. Rev. Food Sci. Food Saf., 2010, 9 (5), 552–571, DOI: 10.1111/j.1541-4337.2010.00126.x.

[19] JILDEH T.R., OKOROHA K.R., MARSHALL N.E., ABDUL--HAK A., ZENI F., MOUTZOUROS V., *Infection and Rerupture After Surgical Repair of Achilles Tendons*, Orthop. J. Sport. Med., 2018, 6 (5), 1–5, DOI: 10.1177/2325967118774302.

[20] KRAUTHAMMER T., *Accuracy of the finite element method near a curved boundary*, Comput. Struct., 1979, 10 (6), 921–929, DOI: 10.1016/0045-7949(79)90061-0.

[21] LAWRENCE T.M., WOODRUFF M.J., ALADIN A., DAVIS T.R.C., *An assessment of the tensile properties and technical difficulties of two- and four-strand flexor tendon repairs*, J. Hand Surg. Am., 2005, 30 (3), 294–297, DOI: 10.1016/j.jhsb.2005.01.003.

[22] Letters P., O.T. Phase, S. Distributions, A.F. Office, *Calcium phosphate polymer composite and method*, 1968.

[23] MakeItFrom, *Polyglycolic Acid (PGA, Polyglycolide)*. https://www.makeitfrom.com/material-properties/Polyglycolic-Acid-PGA-Polyglycolide (Accessed: 14 January 2021).

[24] MakeItFrom, *Polylactic Acid (PLA, Polylactide)*. https://www.makeitfrom.com/material-properties/Polylactic-Acid-PLA- Polylactide (Accessed: 14 January 2021).

[25] MAO W.F., WU Y.F., ZHOU Y.L., TANG J.B., *A study of the anatomy and repair strengths of porcine flexor and extensor tendons: Are they appropriate experimental models?*", J. Hand Surg. Eur., 2011, 36 (8), 663–669, DOI: 10.1177/1753193411414117.

[26] MatWeb, *Overview of materials for Polylactic Acid (PLA) Biopolymer*. http://www.matweb.com/-search/DataSheet.aspx?MatGUID=ab96a4c0655c4018a8785ac4031b9278 (Accessed: 14 January 2021).

[27] MatWeb, *Polyglycolic Acid (PGA)*; http://www.matweb.com/search/DataSheet.aspx?MatGUID-=217394aba5b3413b9fbc034c45310996 (Accessed: 14 January 2021).

[28] MISHRA V., KUIPER J.H., KELLY C.P., *Influence of core suture material and peripheral repair technique on the strength of Kessler flexor tendon repair*, J. Hand Surg. Br., 2003, 28 (4), 357–362, DOI: 10.1016/s0266-7681(03)00080-9.

[29] NAYAK A.N., NGUYEN D.V., BRABENDER R.C., HIRO M.E., MILES J.J., SMITHSON I.R., SANTONI B.G., STONE J.D., HESS A.V., *A Mechanical Evaluation of Zone II Flexor Tendon Repair Using a Knotless Barbed Suture Versus a Traditional Braided Suture*, J Hand Surg Am. 2015, 40 (7), 1355–1362, DOI: 10.1016/j.jhsa.2015.04.009.

[30] Objet, *Objet VeroWhitePlus FullCure® Vero 835,* 2010.

[31] OCHEN Y., BEKS R.B., VAN HEIJL M., HIETBRINK F., LEENEN L.P.H., VAN DER VELDE D., HENG M., VAN DER MEIJDEN O., GROENWOLD R.H.H., HOUWERT R.M., *Operative treatment versus nonoperative treatment of Achilles tendon ruptures: systematic review and meta-analysis*, BMJ, 2019, DOI: 10.1136/bmj.k5120.

[32] OLIVA F., RUGIERO C., GIAI VIA A., BALDASSARRI M., BERNARDI G., BIZ C., BOSSA M., BUDA R., BUONOCORE D., CHIANCA V., COLLINA A., DE CARLI A., DE LUNA V., DI LANNO I., DI LORENZO L., DI PIETTO F., DOSSENA M., FANTONI I., FARSETTI P., FINI M., FINOTTI P., FORTE A.M., FOTI C., FRIZZIERO A., GAJ E., GALEONE C., GAMBERINI J., GASPARINI M., INNOCENTI B., LUPARIELLO D., MAHMOUD A., MARSILIO E., MORETTI B., NATALI S., PADULO J., PELLICCIARI L., PERAZZO L., PICCIRILLI E., PICERNO P., RUGGIERI P., TARANTINO U., VADALÀ A., VERONESI F., VERRI M., VETRANO M., VULPIANI M.C., ZAPPIA M., MAFFULLI N., *I.S.Mu.L.T Achilles tendon rupture guidelines*, Muscles. Ligaments Tendons J., 2018, 3, 310–363.

[33] PODICHETTY J.T., MADIHALLY S.V., *Modeling of porous scaffold deformation induced by medium perfusion*, J. Biomed. Mater. Res. Appl. Biomater., 2014, 102 (4), 737–748, DOI: 10.1002/jbm.b.33054.

[34] PRIDGEN B.C., WOON C.Y., KIM M., THORFINN J., LINDSEY D., PHAM H., CHANG J., *Flexor tendon tissue engineering: Acellulari-*

zation of human flexor tendons with preservation of biomechanical properties and biocompatibility, Tissue Eng. – Part C Methods, 2011, 17 (8), 819–828, DOI: 10.1089/ten.tec.2010.0457.

[35] RAIA R.B.W. SU, QUITKIN F.J.H.M., PARISIEN M., STRAUCH R.J.M.P., *Gross and Histological Analysis of Healing After Dog Flexor Tendon Repair With the Teno Fix™ Device*, J. Hand Surg. Am., 2006, 31 (5), 524–529, DOI: 10.1016/j.jhsb.2006.01.006.

[36] RAWSON S., CARTMELL S., WONG J., CARTMELL S., *Suture techniques for tendon repair a comparative review*, Muscles. Ligaments Tendons J., 2013, 3, 220–228.

[37] RAWSON S.D., MARGETTS L., WONG J.K.F., CARTMELL S.H., *Sutured tendon repair; a multi-scale finite element model*, Biomech. Model. Mechanobiol., 2015, 14 (1), 123–133, DOI: 10.1007/s10237-014-0593-5.

[38] SCHUIND F., COONEY W.P., LINSCHEID R.L., AN K.N., CHAO E.Y.S., *Force and pressure transmission through the normal wrist. A theoretical two-dimensional study in the posteroanterior plane*, J. Biomech., 1995, 28 (5), DOI: 10.1016/0021-9290(94)00093-J.

[39] SMITH A.M., EVANS D.M., *Biomechanical assessment of a new type of flexor tendon repair*, J. Hand Surg. Am., 2001, 26 (3), 217–219, DOI: 10.1054/jhsb.2000.0542.

[40] STRATASYS© INC., *Polyjet vero white plus*, 2013.

[41] STRICKLAND J.W., *The scientific basis for advances in flexor tendon surgery*, J. Hand Ther., 2005, 18 (2), 94–110, DOI: 10.1197/j.jht.2005.02.013.

[42] TANG J.B., *Outcomes and evaluation of flexor tendon repair*, Hand Clin. 2013, 29 (2), 251–259, DOI: 10.1016/j.hcl.2013.02.007.

[43] US C, MORRISS A., PIPER J.H., GRAY D.L.A.R., US C, Patent Application Publication Pub. No.: US 2005/0119694 A1, 2005.

[44] WADA A., KUBOTA H., MIYANISHI K., HATANAKA H., MIURA H., IWAMOTO Y., *Comparison of postoperative early active mobilization and immobilization in vivo utilising a four--strand flexor tendon repair*, J. Hand Surg. Am., 2001, 26B (4), 301–306; https://doi.org/10.1054/jhsb.2000.0547

[45] WIIG M., OLMARKER K., HÅKANSSON J., EKSTRÖM L., NILSSON E., MAHLAPUU M., *A lactoferrin-derived peptide (PXL01) for the reduction of adhesion formation in flexor tendon surgery: An experimental study in rabbits*, J. Hand Surg. Eur. 2011, 36 (8), 656–662, DOI: 10.1177/1753193411410823.

[46] WU T.T., WU P.T., LEE S.Y., WU K.C., SHAO C.J., CHERN T.C., SU F.C., JOU I.M., *Effect of metacarpophalangeal joint position on A1 pulley and flexor digitorum tendons in trigger digit*, J. Chin. Med. Assoc., 2019, 82 (10), 778–781, DOI: 10.1097/JCMA.0000000000000165.

[47] YUNBING W., *Implantable medical devices fabricated from block copolymers*, 2015, EP2203197B1.

[48] ZATITI S.C., MAZZER N., BARBIERI C.H., UNIT H.S., VOLUME E., *Mechanical Strengths of Tendon Sutures*, J. Hand Surg. Am., 1998, 23B (2), 228–233, DOI: 10.1016/s0266-7681(98)80181-2.